Engineering Structures 206 (2020) 109690

Contents lists available at ScienceDirect

Engineering Structures

journal homepage: www.elsevier.com/locate/engstruct

Structural assessment of iron tie rods based on numerical modelling and experimental observations in Milan Cathedral

Grigor Angjeliu[a,*], Dario Coronelli[a], Giuliana Cardani[a], Thomas Boothby[b]

[a] Department of Civil and Environmental Engineering, Politecnico di Milano, Milan, Italy
[b] Department of Architectural Engineering, Pennsylvania State University, University Park, PA, USA

ARTICLE INFO

Keywords:
Iron tie rods
Masonry
Finite element modelling
Experimental observations
Soil-settlements
Historical building
Simulation
Maintenance

ABSTRACT

Iron ties contribute to the stability of structural systems having vaults and arches. The axial force in the iron ties is not easily to be measured but this knowledge is important for assessing the safety of these members. In the case of breakage of iron tie rods, the assessment study needs to understand the causes of the failures. Experimental data are collected, and models are used for their interpretation. The aim of this paper is to propose a new integrated experimental and numerical approach for the structural analysis of tie rod tensions in historical buildings.

The study considers an application at Milan Cathedral, where recently some iron tie failures were observed. The collected data taken into account are: (a) Point cloud measurement of the geometry (b) Understanding of construction phases, (c) Soil-settlement measurement in the last 50 years, (d) Experimental measurement of the iron ties axial force, and (e) Documentation of damage and iron tie failures in the last century. It is here proposed to use an advanced numerical model for simulating, interpreting and predicting the measured response of the iron ties. The finite element numerical model includes detailed geometry of elements, material properties of masonry based on texture observations and iron ties modelling.

The paper shows how the actual structural configuration, the choices on material properties, the consideration of construction stages or load history and soil settlements affect the tension state in the iron ties. In particular, it is demonstrated through the carried-out analysis the possibility to correlate the tension force in the ties with soil settlements. Finally, the developed numerical model can be used also during practical maintenance operations of iron tie replacement, by predicting the stressed state, the possible lateral displacements of the pier and the associated structural safety.

1. Introduction

The behaviour of historical masonry buildings, is widely studied by many authors, among others Heyman [1], who expresses the idea that the stability of these buildings is guaranteed by the geometry of the structure, articulating the term Stone Skeleton. However, in contrast to that, many studies evidence the massive use of iron [2–4]. The registers of the historical buildings construction report the use of a large amount of iron [4]. The iron tie-rods have been and still are used to perform functions of connection, containment and strengthening of the masonry structures. They can have an active role, absorbing the thrusting actions coming mainly by arches and vaults, or a passive role, adopted as a static reserve, as the thrust had to be firstly absorbed by the masonry structure. They were inserted during construction or added later after a damage occurred. In some buildings of the Middle Ages located in seismic areas, where iron was less available, wooden tie rods were used during the construction of masonry structures.

By the 15th century it was quite customary to use tension bars of iron to take the thrust of arches and vaults [5]. Its applications include the use within masonry as an embedded material improving its local mechanical characteristics, or as a structural element "iron tie" to balance the lateral thrust of the arches. Only around the 16th century, thanks to the increasingly widespread use of manuals, that the written evidence of lateral thrust control on masonry began to appear: as mentioned in treatises like the one of Francesco Di Giorgio Martini (1503) and of Leon Battista Alberti (1565) [6].

In particular the use of the iron tie rods is noted to improve significantly the performance and the safety of historical masonry buildings in service conditions [7] or during seismic events [8]. In many historical buildings tie-rods are much diffused as anti-seismic device to

* Corresponding author.
E-mail address: grigor.angjeliu@polimi.it (G. Angjeliu).
URL: http://www.polimi.it (G. Angjeliu).

https://doi.org/10.1016/j.engstruct.2019.109690
Received 28 January 2019; Received in revised form 12 August 2019; Accepted 16 September 2019

prevent the overturning of the walls, to avoid the overturning of the facades, and to anchor firmly the main beams of the floors to the masonry [9]. The effectiveness of tie-rods is widely stressed in many past earthquakes and they are still used today for strengthening, given that their use is considered as a compatible structural intervention [10].

The aim of this paper is to understand the causes of the measured tension force in iron tie rods by the use of advanced structural numerical model. The development of a cause - effect relationship, between external actions and axial force in the iron ties rods, will help also to interpret the measurements achieved during the in-situ investigation, which is further directly connected with the evaluation of the system safety and the actual distribution of forces in the structure. Iron tie failure and consequently redistribution of the forces was documented at the Milan Cathedral [11–14].

The measurement of the axial force in an iron tie is based on static or dynamic procedures [15,16]. The dynamic procedures are based on the modal identification of frequencies of the tie rod, measured experimentally. It typically considers a beam of uniform section, spring-hinged at both ends and subject to an axial force. The identification of the axial force in the tie is performed by the matching a sufficient number of natural frequencies measured experimentally with the same number of frequencies calculated numerically [17,18]. In particular, the influence of unknown boundary conditions, geometric variations of the tie cross section, elastic properties or measurement errors in the accuracy of the axial force identification are widely studied in the literature [18–21]. Example of successful applications include the works of Garziera and Collini [22–24] studying Parma Cathedral and castle of Fontanellato or Vasic and Gentile et al. [12,25] at Milan Cathedral, by estimating the tensile force in most of the tie-rods.

Measurement of forces and stresses in a system creates a new prospective for an analysis of the real mechanical state of an existing structure. Although the difficulties during practical experimental measurement due to work at considerable heights, the investigations of the state of stress is frequently performed. However, it is not always easy to interpret the measurement results, due to the influence of many factors (level of stress, defects, anchorage system and non-visible damage).

Within the specific aims of this paper, the method proposed here is used to interpret the experimental measurements, by taking into consideration the influence of the accurate geometric configuration of the system, documented structural evolution in time, and settlements, with the possibility to make predictions about the future state of stress on new loading conditions e.g. during maintenance operations (iron tie replacement) or new events e.g. possible settlements or seismic loading.

It is of great interest to estimate which part of the thrust is balanced by the ties and which part is balanced by the buttressing system. Understanding of the level of tension in the iron ties is directly related to the evaluation of the statics of the structure and its current safety [8].

In this paper we will investigate the structural assessment of iron tie rods by the integration of finite element model and experimental observations applied in a very complex building like Milan Cathedral [14,26]. The choice of this case study is discussed in Section 3. It is related to the high number of iron tie rods present in the building since its construction as well as the concerns of the monument safety after the failure of a number of iron ties in the recent years [27]. Considerations and assumptions of the developed numerical model are discussed in Section 4. In Section 5, the results of the analysis carried out for a single bay are reported, studying the tension forces of iron tie rods in function of the load history, self-weight and soil settlements. Moreover, a practical maintenance operations of iron tie replacement is considered. The numerical model shows a good performance by predicting the pier top lateral displacement during this operation. Finally, in Section 6 the results obtained in the previous section are discussed in the light of the interpretation of the causes of iron ties failures in the naves of Milan Cathedral, in relation to their position, tensile force measured experimentally and the complex documented history.

2. Structural assessment of historical masonry buildings with iron tie rods

The estimation of the axial force in the iron ties through the structural analysis in the case of historical masonry construction deals with many uncertainties: it includes complex geometry of structural elements (buttress, pier, wall, arch, vault, flying-buttress, etc.), their connections, mechanical properties resulting from the varying texture of masonry. Ageing and a long history of construction, loads and interventions, may be only partially described or even unknown [14].

Moreover, increasing phenomena of corrosion and local damage, are present in these elements due to the long history of the building, reducing though their capacity to balance the lateral thrust and might cause failure of these elements, redistribution of forces, consequently putting into discussion the structural safety. A multidisciplinary investigation of the technology of production of the iron ties reveals difficulties related to the non-homogeneous section of the iron-ties, the presence of defects, degradation, and the difficulty in inspecting the anchorage part [13,28,29]. Furthermore, the same studies mark the presence of defects as well as their influence on observed failures in-situ.

Under these conditions, visual observations of damage, observation of masonry texture, measurements of complex geometry, measurement of the axial force in the iron ties or the state of stress in masonry, are important evidence for making an approximation of the real mechanical state [14,26].

Integration of the experimental observations techniques with advanced numerical model is a viable solution to improve detailed numerical prediction capabilities. At the present state numerical models are poorly developed in this direction. Within the aim to estimate numerically the axial force in the iron tie rods of Milan Cathedral, Vasic [12] tried to develop a finite element prediction, but did not investigate the correlation with the soil settlements.

The results of the current research presented in this paper highlighted the need to develop more advanced numerical models. In particular, the necessity to consider more complex geometry, internal divisions among structural members as well as accurate inspection and modelling of iron ties anchorage. It was essentially the need to formulate a new comprehensive finite element model based on the above stated requirements and criteria.

3. Model of Milan Cathedral

The aim of this section is to describe the collected experimental data and their use for developing an accurate Finite Element (FE) model of the naves of Milan Cathedral, in order to provide interpretation for the recent observed tie rod failure [27], prediction of the measured tension state in the ties and evaluation of the system safety.

3.1. Overview

The construction of Milan Cathedral started in 1386 from East to West with the apse and choir [11,30,31]. It has the shape of the Latin cross with one nave and four aisles. The cross dimensions in plan are

a) b)

Fig. 3.1. Milan Cathedral: (a) South-West view of Milan Cathedral, (b) Iron tie rods inside the church.

88 m × 157 m. The late Gothic monument is noted also for the extensive use of the pink marble from the quarries of Candoglia (near Lago Maggiore) and the presence of iron tie rods dating from the construction time (Fig. 3.1). The apse has a half octagonal shape, while the Tiburio over the crossing has a full octagonal shape.

The height of the nave is 45 m to the crown and its width is 19.2 m that is the double span compared to the two aisles, which are 30 m and 23 m high respectively (Fig. 3.2). The separation of the nave from the aisle is effected by large piers, 31 m height. Their shape is defined by the cross-section of the ribs and arches, inscribed in a circle with a diameter of 2.55 m, except for the four piers that support the great cupola (Tiburio) which have a larger diameter, 2.95 m. Piers are connected to each other by pointed arches. The double vaulted system over them, characteristic of the cathedral, is composed by the ribbed vaults, the barrel vaults over them, as well as a heavy stone roof laid over the whole. The wall over the arches defines a diaphragm wall, that balances the horizontal thrust of the arches, together with the iron ties. The thrust is further transferred to the ground by the pier and buttressing system with an important contribution of permanent iron tie rods, which are the object of investigation in the present research.

3.2. Experimental observations and model development

The data collected during the research were obtained from different sources: geometry (available drawings and point cloud measurement based on photogrammetry), visual observations, crack pattern survey (present and old), monitoring system data (vertical and horizontal displacements of some piers), NDT testing of iron ties, archive research (structural system evolution, historical damage).

3.2.1. Geometry survey and modelling

Starting from the geometric survey and on-site observations extended over two years, a 3D FE continuum model was created. The model considers a typical bay of Milan Cathedral [14]. This engineering choice is related to the main force flow in the structural system, with the transfer of the thrust in the transverse North–South direction.

The numerical model was developed in accordance with the strategy developed by Angjeliu et al. [26,32] which considers a detailed assembly of structural elements and automatic reconstruction procedures for the most complex parts of the analysed typical bay e.g. nodal zones and ribbed vaults [33]. Direct observations in situ show that these components are the most complex elements of the system, hence also the most time consuming during structural modelling. The parametric model is based on known or deduced rules and relationships and implemented applying principles of computational geometry. Different models can be generated by the variation of the inputs in the parametric model [33,34]. The masonry vaults created through a parametric model proposed by Angjeliu et al. [33], are shown in Fig. 3.3 and include the tas-de-charge, web, ribs, arches and rubble-fill.

The final assembly of the finite element structural model considers the three-dimensional configuration of the Cathedral using 3D solid geometry, discretized with reduced order linear tetrahedral elements. Approximately the model consists of a total of 750000 nodes. The complete model is rather complex, as it includes detailed geometry of each member (Fig. 3.4). In the main assembly the main structural elements are considered: the piers, the buttresses, the masonry vaults with all of its components, the iron ties with their anchorage and the walls that act as buttressing. Moreover, the model considers also secondary structural elements: the barrel vault (sordine) and the flying arch. Correct modelling of each of these parts is important in order to represent the correct stiffness of each structural element.

3.2.2. Anchorage detail and modelling

Inspection of the cathedral shows that the exterior anchorage is located within the buttress (Fig. 3.5a) and not in the pier as believed previously [12]. Three elements can be observed: (1) the iron tie, (2) the wedge, and (3) the stone block where the tie tension force is transmitted (Fig. 3.5b). The developed numerical model implements the main characteristics of the observed load transfer mechanism: from the iron tie to the stone block (element 3) and then to the surrounding masonry of the buttressing wall (Fig. 3.5a). It was chosen here to model the stone block with an elastic material, in which is embedded a part of the iron tie rod (Fig. 3.5b). The advantage is to have a robust numerical solution with no localization phenomena

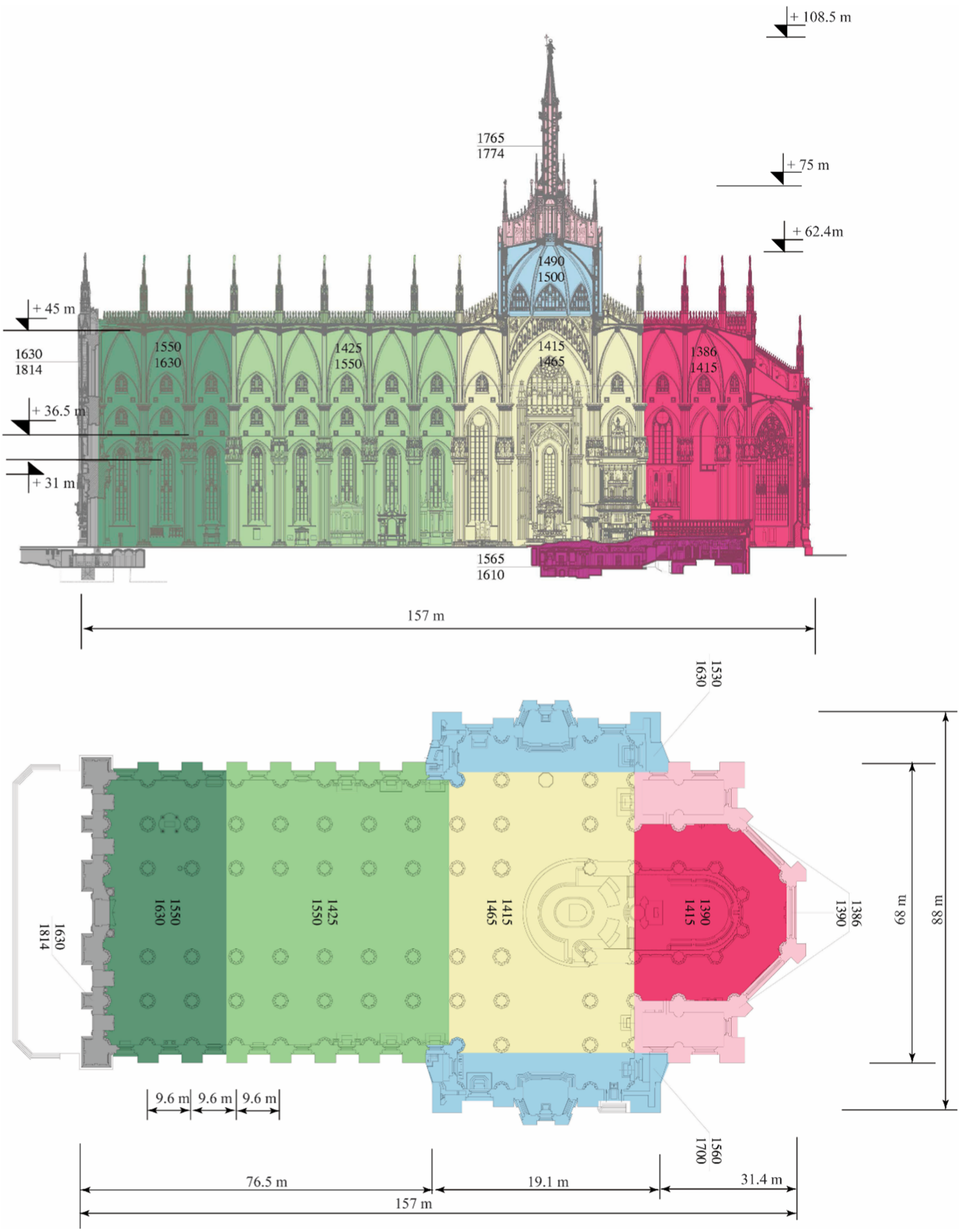

Fig. 3.2. Plan and longitudinal section of Milan Cathedral with construction phases. *Courtesy of the Veneranda Fabbrica del Duomo di Milano (VFD).*

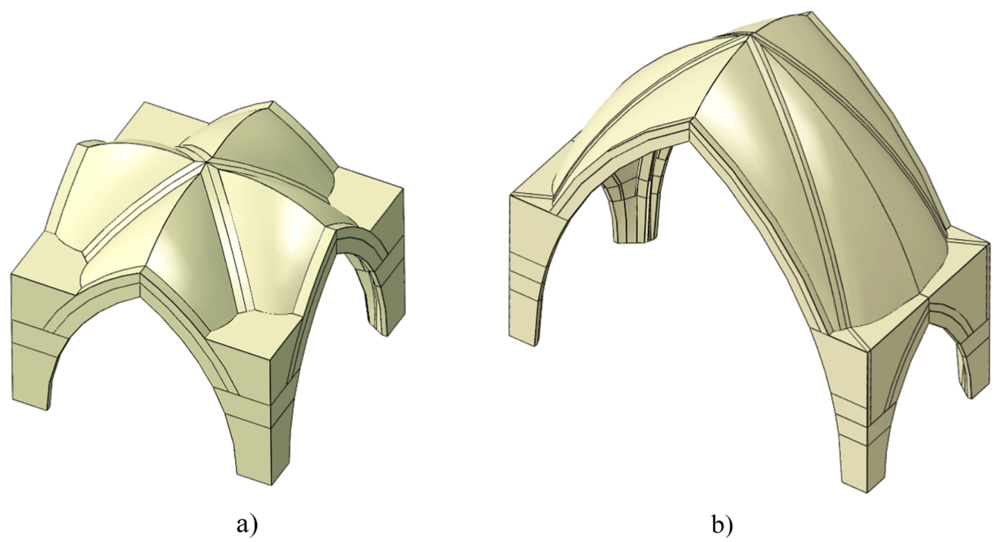

Fig. 3.3. Automatic generated digital models of the vaults in Milan Cathedral: (a) aisle, (b) nave.

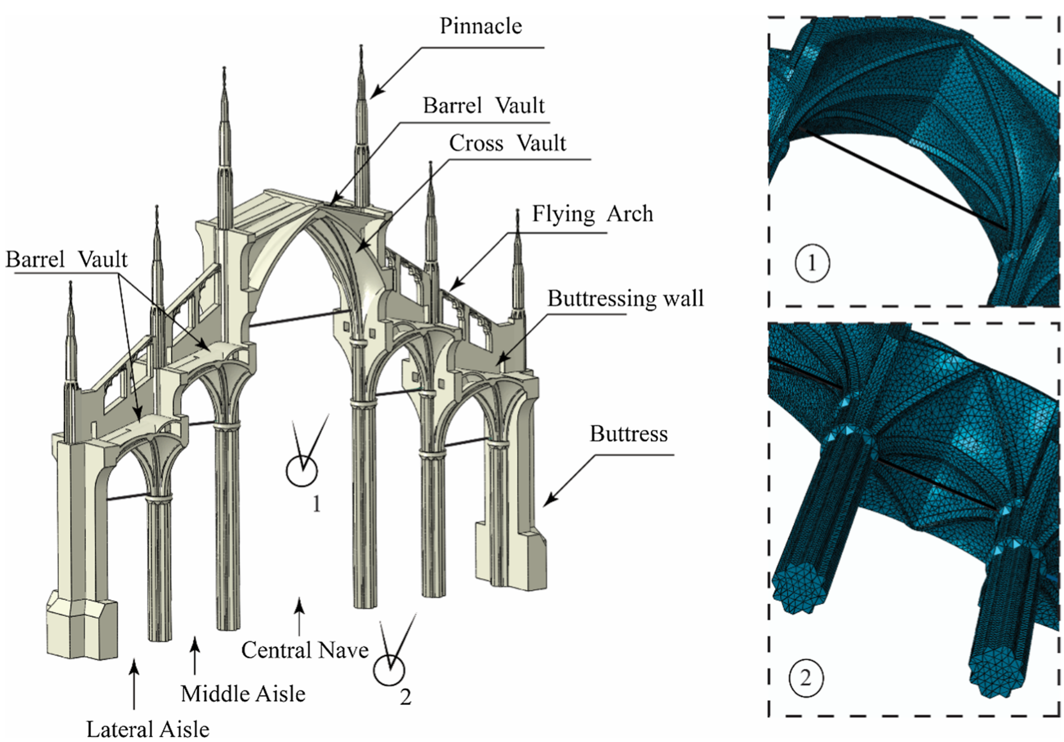

Fig. 3.4. Numerical finite element model of a typical bay of Milan Cathedral.

inside the block and a good transfer mechanism to the surrounding masonry similarly to what observed. Moreover, failure mechanisms are typically observed in the iron ties, while there are no documented cases of failure in the stone masonry part of the anchorage system (Fig. 3.5) [14]. We note here the importance of inspection of the anchorage of iron tie rods [29]. If important damage is found, then the numerical model should be updated accordingly, by modifying the elastic properties of the embedded part (Fig. 3.5b).

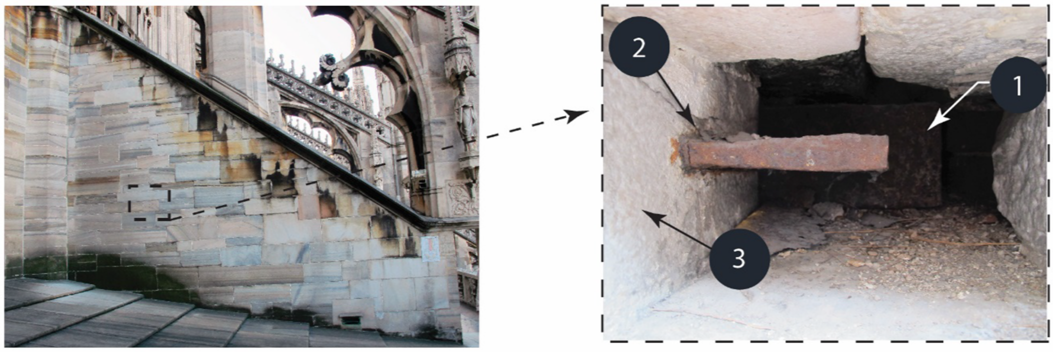

a)

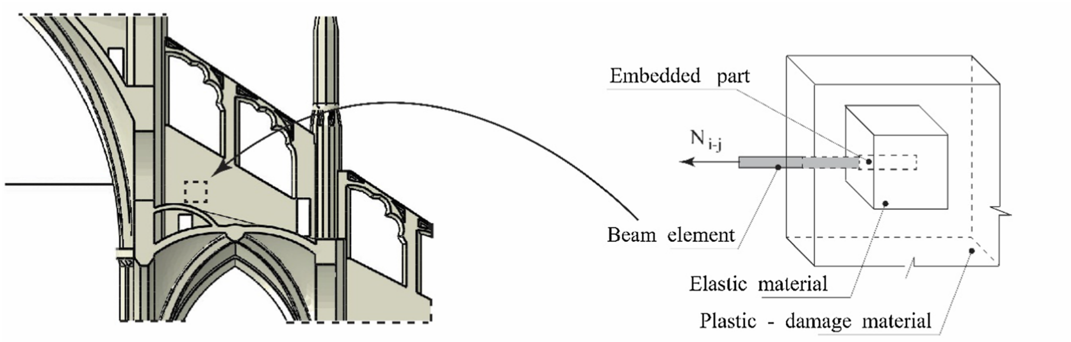

b)

Fig. 3.5. Anchorage detail: (a) Anchorage location within the buttressing wall, (b) Finite element 3D modelling of anchorage detail.

3.2.3. Iron ties investigation

The presence of the tensile force in the ties results clearly from its position as well as from the observed failures. Recently, two failures were recorded in the nave ties of the 6th bay (2009), and 3rd bay (2011), arousing great concern about the statics and the safety of the cathedral (Fig. 3.6, – see also Fig. 3.7c).

Further research in the Veneranda Fabbrica del Duomo di Milano (VFD) archive showed that a series of other iron tie failures was documented in the cathedral before 1960s (Fig. 3.7) [11], linked to the lowering of the water table at the beginning of the 20th century in the city of Milan (see Section 3.2.4).

Tests to quantify the experimental values of the axial force, mechanical properties of iron, presence and influence of the defects were performed by Vasic [12] and Bellanova [13,29]. The iron ties are not perfectly alike to each other, with some variation in their cross-section dimensions, owing to the technology of iron production. In the present study they were modelled with an average dimension of 55 × 75 mm. The yield stress is estimated between 150 and 200 MPa, corresponding to a yield force of 620–825 kN [11], although in reality, failure could occur also at lower values of force owing to local defects present in the metal.

Dynamic identifications tests performed on the tie rods in the cathedral confirmed the existence of the tensile axial force [12,25], as expected. In this application, the numerical identification procedure considers a beam with uniform section, subject to axial force and spring-hinged at both ends.

Here, the focus is on the experimental measurements of the iron tie tension force in the nave and aisle, although the data are available for most of the cathedral. The measurements performed by Vasic [12], regarding the transversal direction in the first 7 bays are plotted in Fig. 3.7a, b. Only a few of the measurements are missing due to the presence of heavy objects (e.g. lanterns or electric cables) on the iron ties which would corrupt the dynamic measurement results. The results of the tests are rather scattered demonstrating clearly the influence of other effects beside the structural configuration.

Finally, in the 6th bay it is noted how the recent failure in 2011 of one of the iron ties ($T_{2\text{-}3}$) in the aisle (with a value close to zero in

a)

b)

Fig. 3.6. Documentation of iron tie failures: (a) Failure of the iron tie (6th bay T 2-3) [12], (b) Crack in the iron tie (3rd bay, T 2-3) [12].

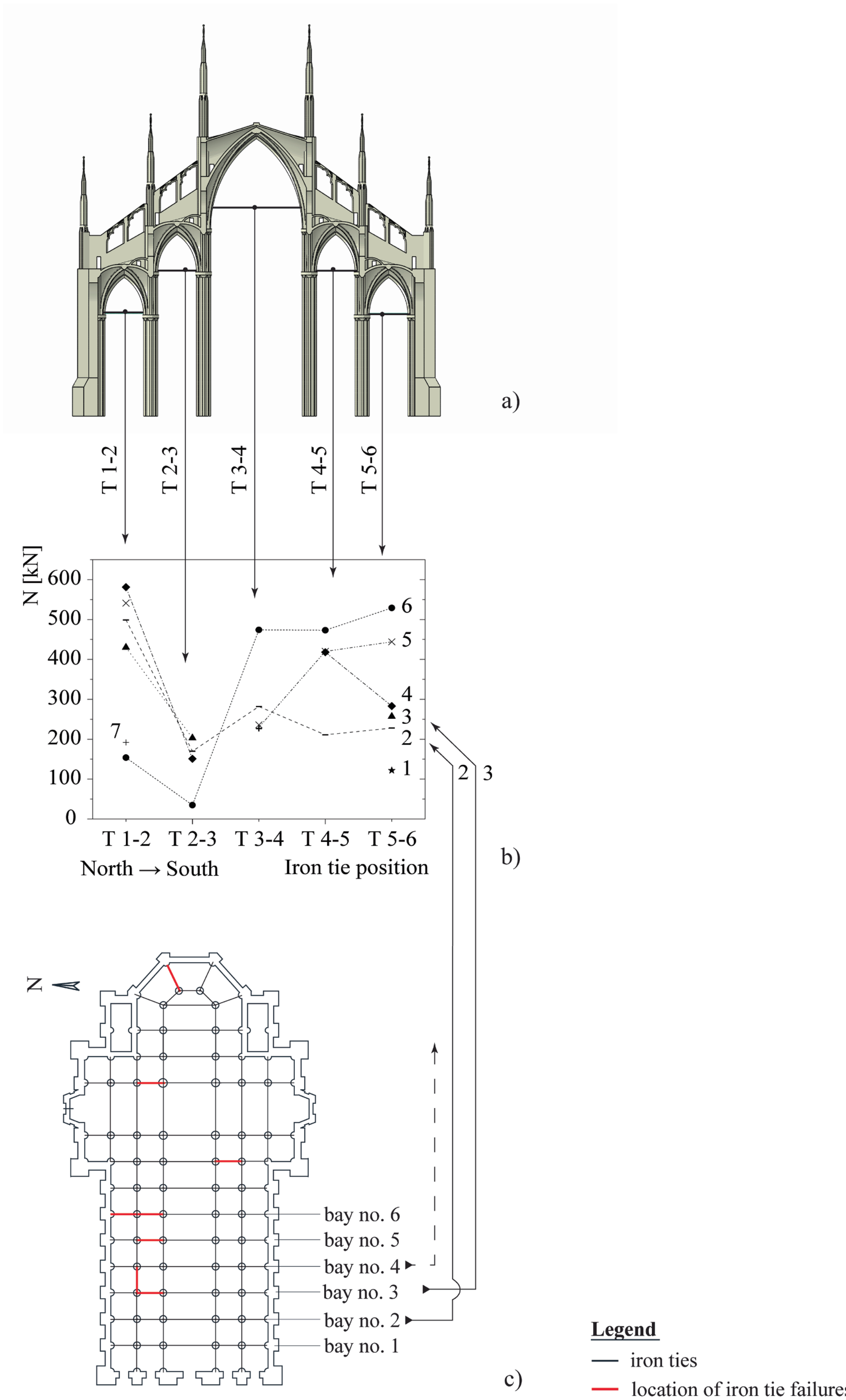

Fig. 3.7. Iron tie rods (a) Location of the measured ties in the cross section, (b) Experimental values of the axial force in the iron tie rods from [12], (c) location of iron tie failures.

Fig. 3.7b, c), has created a jump of the state of stress in the central nave with respect to the other values. Hence this value will not be considered in the following computations as judged to be misleading due to the recent observed failure.

3.2.4. Settlement study

The investigation carried out to identify external causes in the long history of the building, influencing the tensile force in the iron ties, showed beside others the importance of differential settlements. Major events occurred over centuries of life, among which: the building of the nave, the stone roof, and the subsidence in the 20th century. In the history of the cathedral, the lowering of the water table in the 20th century due to industrial activities in Milan and the associated subsidence effects caused redistribution of internal forces and heavy damage to a great number of piers, as well as in the vaulting [35]. The cause of the observed differential settlements in the cathedral can be found in the 25 m reduction [36] of the level of the water table (Fig. 3.8a). As clearly noted in Fig. 3.8 most of the settlements happened before the year 1965. In fact, Ferrari da Passano, Architect of the VFD at the time, documented significant damage around the area of the Tiburio, such as wide cracks in piers and vaults.

In order to control the settlements, a permanent monitoring system of the pier settlement and top horizontal movements was installed in 1966 [37]. Excluding the Tiburio and the apse, not analysed in this paper, the elaboration of the results showed areas of strong settlements in the successive years in the naves of Milan Cathedral (Fig. 3.8b). In particular were noted strong differential settlement in the north of the naves as well as a discontinuity line in the 4th bay probably connected with a historical construction joint.

As far as the nave is concerned, the internal piers are supported on isolated foundations while the perimeter walls (buttress) are supported on continuous foundations. The average level of the foundations with respect to the cathedral floor is at a depth of 7.4 m. The soil is composed mainly of gravel and sand with traces of silt, and in part by layers of sandy clay silt to a depth of 100–120 m as described by Niccolai [38]. The asymmetric settlements are connected also with the mechanical characteristic of the soil, e.g. the presence of a layer of silt and clay at a depth of 9–11 m [11,38]. Coronelli et al. [35] demonstrated through numerical analyses, this layer to significantly influence the foundation settlements in cases of subsidence.

In the following, the focus will be on the settlement mechanisms as one of the main identified external causes, threatening the safety of the system, with the aim of interpreting and quantifying its effects in the axial force evolution in the iron tie rods. Other secondary factors may include temperature, or local defects in iron ties.

4. Numerical analysis

In this section, the choices regarding the structural analysis are briefly discussed, numerical implementation of the finite element method, constitutive law and the mechanical parameters for historical masonry.

4.1. Formulation of the numerical model

The problem considers a quasi-static analysis, small deformation and small displacement assumption. The numerical solution of the governing equations is sought as a function of space and time $\boldsymbol{u}(\boldsymbol{x}, t)$. The nonlinear constitutive equation described in the following section, being elasto-plastic is dependent on the loading path. Thus, the stress field $\boldsymbol{\sigma}(\boldsymbol{x}, t)$ depends on the history of other variables at the same location $\boldsymbol{x}$. The computation of the elastoplastic response follows the description of the time stepping procedure, the discretization approach, the integration of the constitutive relationship based on an implicit scheme, while the global equilibrium of the structure is treated with a Newton iterative method according to the description of Hibbitt, et al. [40]. The formulation considered here is a displacement based approach [41] where the displacements $\Delta\boldsymbol{u}_n$ as the primary unknown variable.

4.2. A constitutive plastic-damage model for continuum

In a macroscopic approach, the computation of masonry mechanical properties as a homogenized periodic medium results cumbersome due to the heterogeneous nature of units and mortar distribution in the assemblage of a historical masonry. Hence the assumption of periodicity of the internal structure necessary for the homogenisation process does not hold anymore in this case. Therefore, the discussion in the present work follows a detailed division between parts to consider the internal heterogeneity of historical constructions in line with in-situ observations. The model considers an isotropic model for each part/element, but different parts have different stiffness and strength properties. This provides a better approximation of the physical reality than what would be obtained with the same isotropic and homogeneous model in all parts/elements.

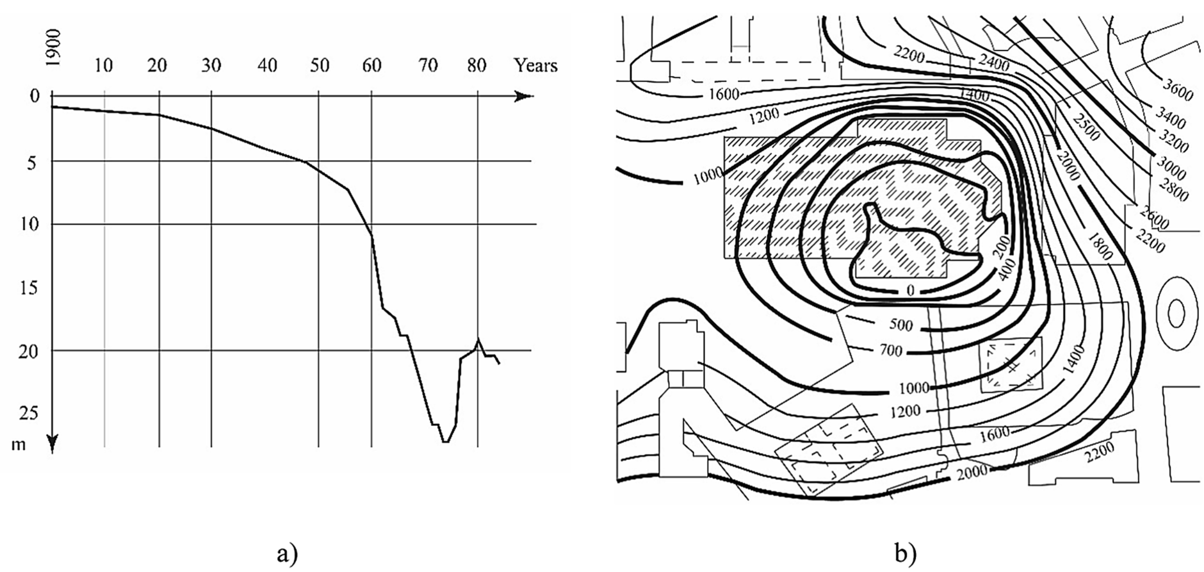

Fig. 3.8. Lowering of water table and its effects on Milan Cathedral: (a) Measurements of lowering of the water table in Milan [36], (b) Measurement of differential soil settlements due to subsidence in the period 1969–1980, in 100 × mm [39].

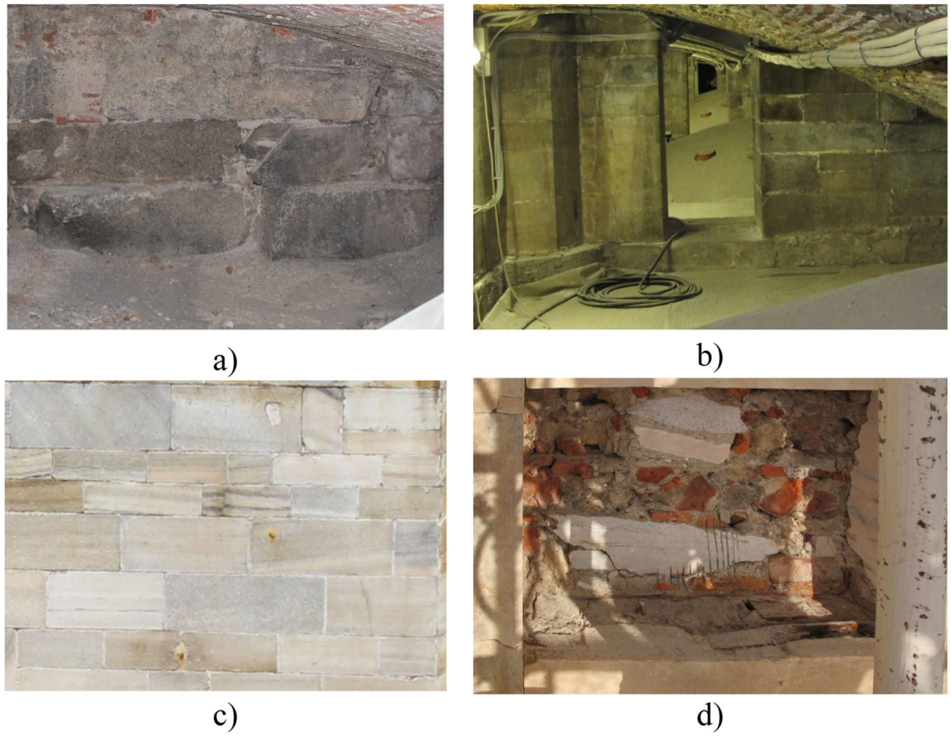

Fig. 4.1. Example of masonry typologies in the Milan Cathedral: (a, b) Regular cut stone-masonry, (c, d) Three leaf masonry made with Candoglia marble and bricks.

4.2.1. Constitutive model

The formulation of the adopted constitutive model is proposed by Lubliner et al. [42] and further modified by Lee and Fenves [43], implemented in the software Abaqus [40]. Its primary intention is to model concrete structures, but it is suitable in general for quasi-brittle material such as rock or masonry with proper choices for material parameters. The state equation is given as:

$$\boldsymbol{\sigma} = \boldsymbol{E}:(\boldsymbol{\varepsilon} - \boldsymbol{\varepsilon}^{\boldsymbol{p}}) \quad (1)$$

The constitutive model includes the plastic deformations $\boldsymbol{\varepsilon}^{\boldsymbol{p}}$ as internal variable. Furthermore, there is a possibility to define the uniaxial tensile and compressive strength, f_t and f_c. Numerous applications of this constitutive model for masonry structures are considered in the literature [44–46].

4.2.2. Masonry observations and modelling parameters

Direct observation of structural details and inspection of the internal parts of masonry, is a fundamental aspect in the definition of actual divisions within the building. Moreover, certain masonry texture can be associated to certain material mechanical parameters [47]. During the cathedral inspection different types of masonry were observed. The used materials are Candoglia marble, Serizzo stone, clay bricks and iron. Observations show that masonry is made of larger stone blocks in critical locations such as the buttress, the walls over the arches, etc., and with slightly lower dimensions in the other parts. Similar considerations are true also for the percentage of clay bricks in the masonry, e.g. in similar critical locations less brick and more stone elements are usually found (Fig. 4.1).

The collected observations are grouped, based on similar mechanical characteristics, in 5 main representative typologies: (1) Masonry type 1 (i.e. made of mainly of stone blocks, see Fig. 4.1a, b), (2) Masonry type 2 (i.e. a three leaf masonry, where the outer ones are made of regularly cut Candoglia marble while the internal part is a brick masonry with inclusions of stone, see Fig. 4.1c, d), (3) Masonry used for the construction of arches and ribs (i.e. made of large marble blocks with thin mortar joints), (4) Masonry used for the piers (i.e. made of an outer ring of marble and an inner core of Serizzo stone), (5) Masonry for the web of the vaults (i.e. made of clay brick, typically 38 cm thick for the cross vaults and 20 cm thick for the barrel vaults).

It is clear that it would be possible to consider more masonry typologies, but on the other hand this requires further investigation apt to increase the level of knowledge on the historical building object of study. On the basis of the inspections conclusions were drawn on the high quality of masonry, in particular for the piers, arches and ribs.

The mechanical properties are reported in Table 4.1. They are based on extensive inspection carried out in the cathedral and partially on previous experimental work carried out the period between 1960 and 1980 on masonry walls reconstructed in laboratory with a similar technology of construction as the cathedral [11]. Similar mechanical properties are reported also in other Gothic cathedrals, which are noted for a very solid masonry construction technique [48,49]. Moreover, the correlation obtained between numerical results, experimental

Table 4.1
Mechanical material properties adopted for the numerical analysis.

Structural elements	$\gamma\ \left[\frac{kN}{m^3}\right]$	$E\ \left[\frac{N}{mm^2}\right]$	$\vartheta\ [-]$	$f_c\ \left[\frac{N}{mm^2}\right]$	$f_t\ \left[\frac{N}{mm^2}\right]$	$G_f^I\ \left[\frac{Nmm}{mm^2}\right]$	$G_{fci}\ \left[\frac{Nmm}{mm^2}\right]$
Masonry “type 1”	22	4000	0.2	6	0.25	0.015	1.5
Masonry “type 2”	20	2000	0.2	4	0.2	0.012	1.2
Arch/Rib	22	8000	0.2	7	0.35	0.02	1.5
Pier masonry	22	7000	0.2	7	0.35	0.02	1.5
Vault (brick masonry)	18	2000	0.2	4	0.2	0.012	1.2
Rubble masonry fill	16	800	0.2	2	0.15	0.012	0.5
Iron tie	8000	205 000	0.3	200	200	–	–

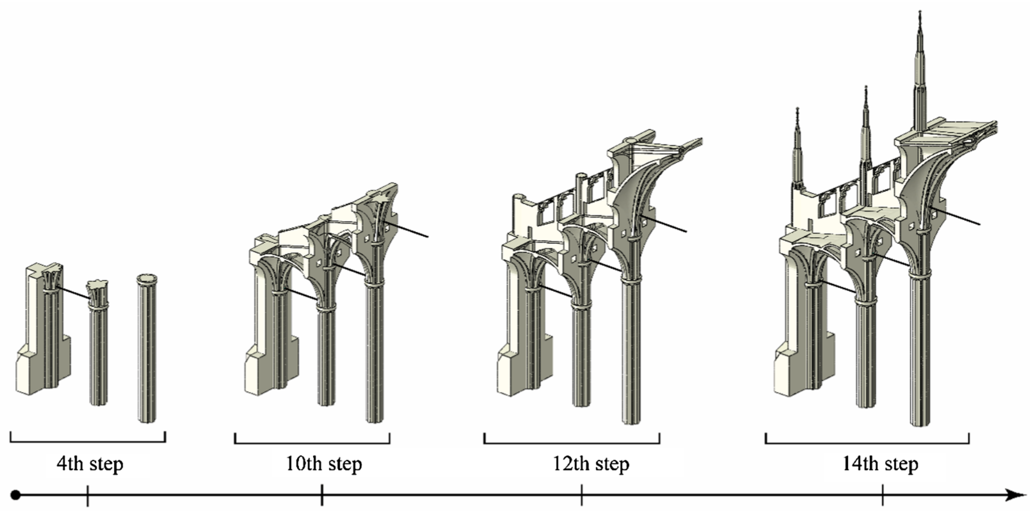

Fig. 4.2. Some of the construction stages considered during the analysis.

observations and displacement measurements, strengthened the confidence about the considered material divisions and the selected mechanical properties (see the following sections).

The constitutive model requires also the definition of the following mechanical parameters:

K_c is the ratio between the magnitude of the deviatoric stress in uniaxial tension and compression. K_c results to depend on the internal angle of friction, which varies in the range $tan\phi = 0.7 - 1.2$, [50] depending on the type of mortar. A typical value is $tan\phi_r = 0.75$, therefore $K_c = 0.667$. Studies of Van der Pluijm et al. [50] or Lourenço [51] demonstrated that the dilatancy angle ψ depends on the confinement level. According to these studies, in the case of masonry, the dilatancy parameter $tan\psi$ may vary from 0.2 to 0.7 for low confinement stress, depending on the roughness of the contact surface. In this study a value of $tan\psi = 0.7$, suitable for low confining pressures is used. The ratio f_{b0}/f_{c0} is the ratio of biaxial to uniaxial compression yield strength. Referring to studies of Page et al., Dhanasekar et al. and Naraine et al. [52–54], the value 1.16 is adopted in the present study.

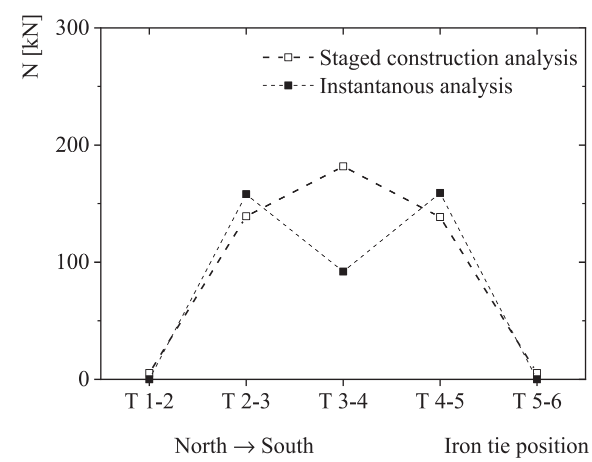

Fig. 5.2. Effect of load history in the axial force due to self-weight.

4.3. Staged construction analysis

The instantaneous application of the loads in the global models is not physical as it does not correspond to the real construction process. An application considering different stages of construction, is shown in the following section to better assess the actual state of stress in the structure as the simulated damage is closer to that observed in-situ, or

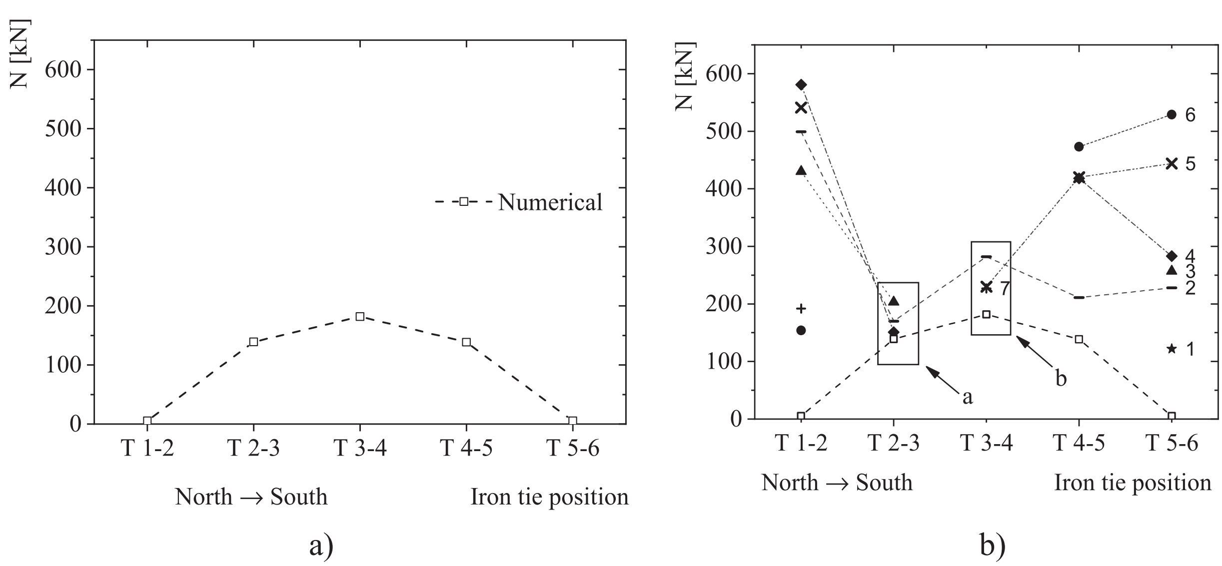

Fig. 5.1. Analysis of tie axial force, *N*, in the self-weight structural configuration: (a) Numerical prediction along a generic transversal section of the nave, (b) Comparison of numerical and experimental values (numbers 1–7 represent the measured bays).

the predicted axial force in the iron tie rods is closer to the experimental measurements. The staged construction analysis is typical in bridge engineering, while its application in historical structures was considered by Roca et al. [48] and Pelà et al. [55].

In the adopted technique, the new elements are added in a stress-free state, in which the new unstressed parts are added to an existing mesh that has already been deformed under previous static gravity loads. The present analysis of the single bay model of Milan Cathedral considers:

(a) Single step analysis (instantaneous)
(b) Multi-step analysis (staged construction).

The first one considers the instantaneous application of loads. The second analysis technique takes into consideration the most important

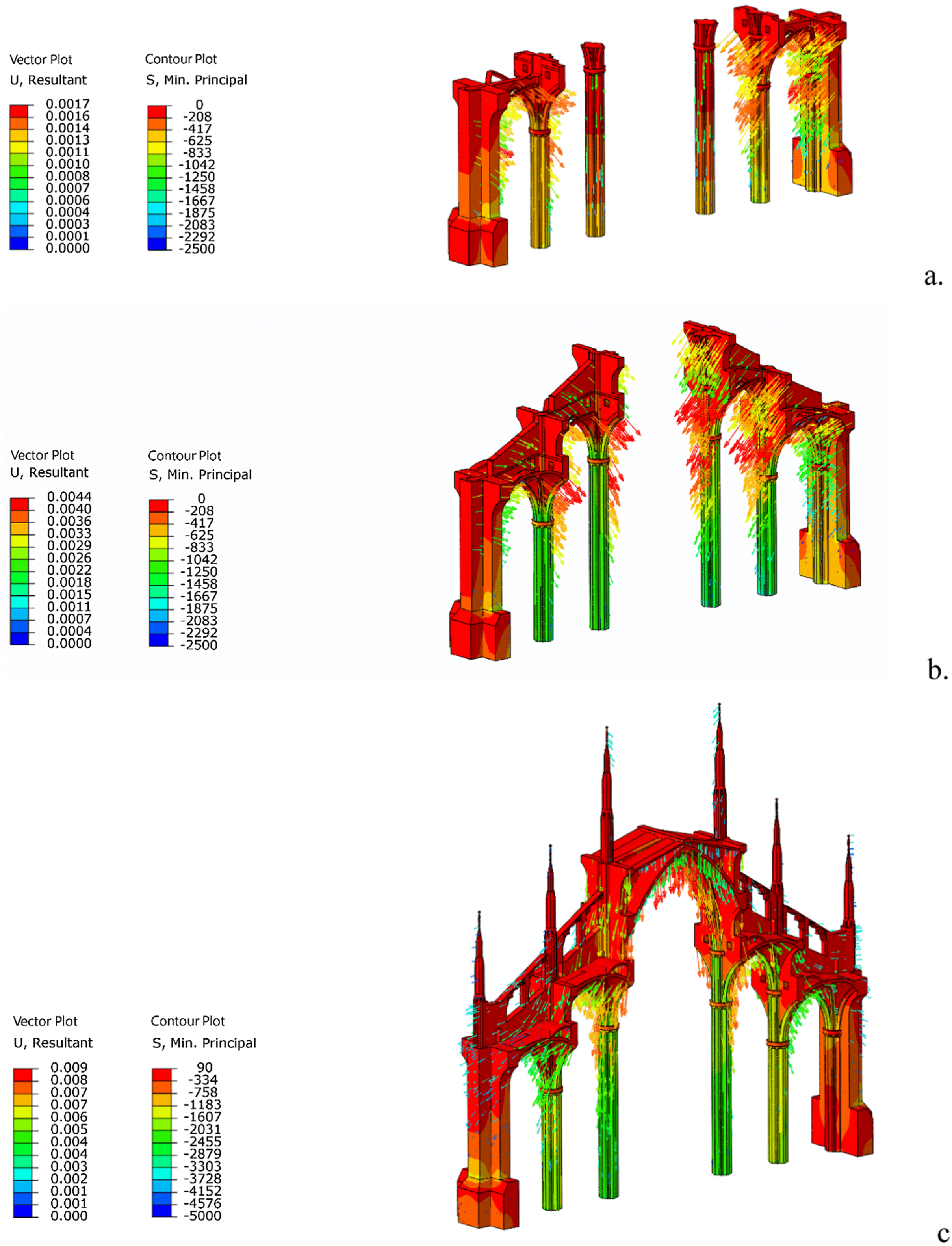

Fig. 5.3. Principal compressive stresses and displacements in different stages of the structural evolution.

phases in the history of construction of the cathedral. The historical research in the technical archive as well as the construction history of other similar buildings [2], suggested that the construction of the cathedral in the transversal direction started from the lateral aisle to the central nave. The construction of the lateral aisle was necessary to balance the thrust of the central nave with a span of 19.2 m. The staged construction analysis is divided in 15 steps, of which 12 consider a change in the geometry of the constructive system (construction of the aisle, arches, vaults, nave, etc.) [26]. Some of the most important stages (for one half of the system) are shown in Fig. 4.2.

5. Modelling results

In this section are discussed the results of the analysis carried out for the Milan Cathedral regarding the structural configuration, staged construction analysis and soil-settlement effects on the tension force in the iron tie-rods.

5.1. Study of the self-weight structural configuration

The values of the axial force, N_{i-j}, due to self-weight analysis (considering staged construction), are plotted in Fig. 5.1a. The differences between the staged construction analysis and instantaneous analysis are described in the next Section 5.2. The predicted data are then compared with the measurements of the axial force in the first 7 bays of the cathedral (Fig. 5.1b). The first comparison with the axial force measurements, N_{i-j} is satisfactory as regards the ties $T_{2\text{-}3}$ and $T_{3\text{-}4}$ (tagged as “a” and “b” in Fig. 5.1b), giving a first confirmation on the accuracy of the numerical model. The axial force values measured in the tie $T_{2\text{-}3}$ are scattered around the value 167 kN close to the numeric self-weight value 139 kN. While the values $T_{3\text{-}4}$ are scattered around the value 227 kN close to the numeric self-weight value 182 kN (Fig. 5.1b). As expected, the results could be only partially related to the self-weight configuration of the structural system, because of the known history of soil settlements (see Section 3) [35]. Even allowing for the symmetry of the construction, the distribution of the tension force in the ties results non-symmetric (Fig. 5.1b). In particular, is noted that the numerical solution shows nearly no tension forces in the side aisle iron ties. The interpretation of these results will be given in the following section and is connected to the evident contribution of the settlements.

5.2. Influence of the load history (staged construction analysis)

The difference noted here in the tie $T_{3\text{-}4}$ is up to 200% of difference when comparing instantaneous and staged construction analysis (Fig. 5.2). The results highlight the necessity to consider the construction stages where a major change of the general trend of displacements or a different development of localization phenomena are to be expected. In our case the most important event is the construction of the central nave. In Fig. 5.3 are plotted the displacement vectors in different phases of the structural evolution. Here is clearly noted the change in the direction of the displacement prior and after the construction of the nave, related to the action introduced after the central nave construction. The consideration of other steps in the analysis shows to be of rather secondary importance.

Besides giving better results in terms of comparison of predicted iron tie forces and level of observed damage, the staged construction analysis in many cases converges to a solution faster with respect to the instantaneous analysis. The interpretation relies on the simulation of the construction process being closer to the reality. This also means less localization phenomena, hence lower computational burden.

5.3. Sensitivity analysis

The sensitivity of the numerical solution of the axial force in the iron ties is tested against the variation of Young’s modulus E_m of masonry and E_i of iron. The mean values of the modelling variables are the ones reported previously in Table 4.1. The Coefficient of Variation (CoV) is equal to 10% for the masonry typology named arch, rib and pier in Table 4.1, while is chosen a CoV = 20% for the other kinds of masonry where less information is available on their internal structure. Similar coefficients of variation are reported also by Augenti and Parisi [56] or recently by Salustro et al [57]. Based on these parameters, a set of random values of the elastic moduli are generated assuming a Normal Distribution with the specific mean and selected variance. A similar procedure is developed also for the iron tie rods, where is considered CoV = 5%, connected with the technology of production of iron tie rods, or the presence of internal defects in the ties as highlighted by previous research by L'Heritier [28], Vasic [12] and Bellanova et al. [13,29]. In particular for the iron ties, the inclusions may affect the response of the material in the non-linear range, but also influence the large standard deviation of the experimental results. The same research highlighted the fact that uniaxial tests showed elastic modulus values comparable to modern steel while significant differences are noted for strength and ductility [58].

In both cases the results confirm the general distribution of the tension force in the iron ties (Fig. 5.4). The major effect of parameters variation is noted in the central nave with a 28 kN dispersion and a CoV = 15.5%. The sensitivity analysis confirms the fact that the variation of material properties

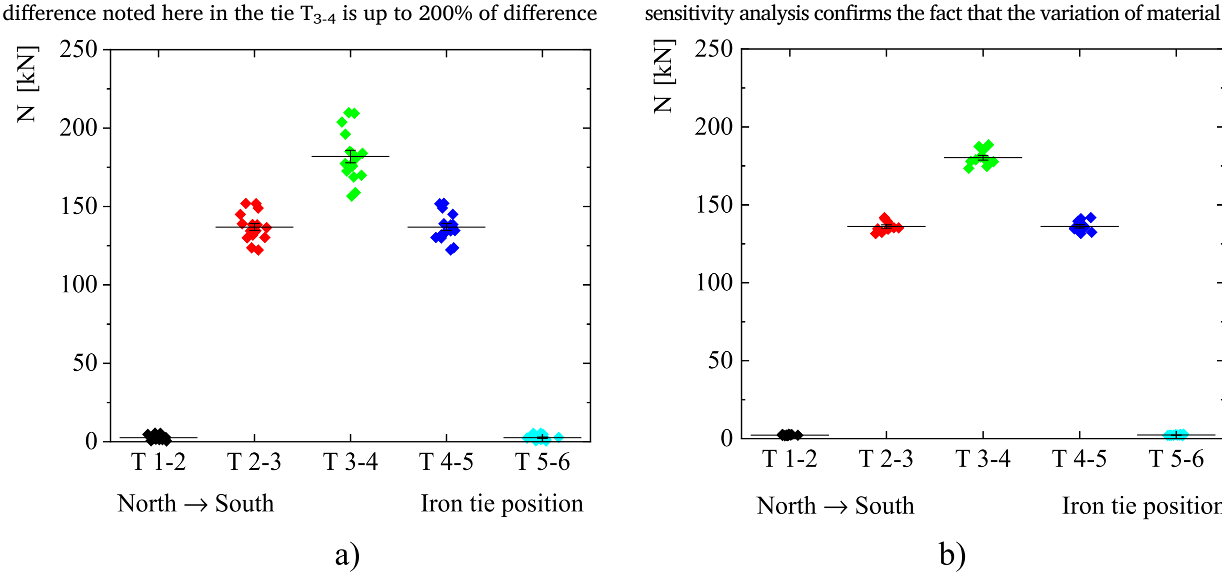

Fig. 5.4. Effect of variation of modulus of elasticity, E, of (a) masonry structure and, (b) iron tie, on the tie tension force N.

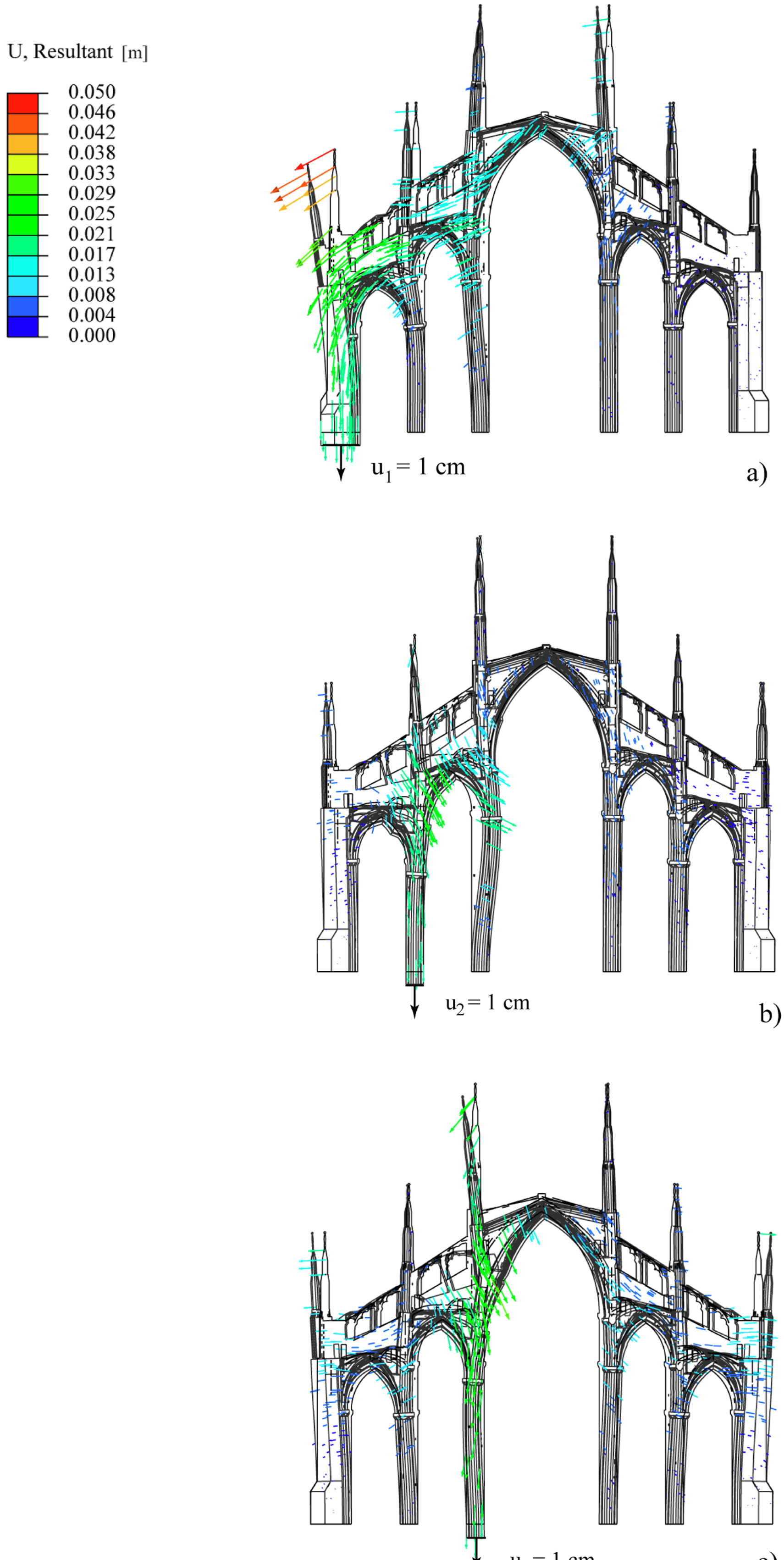

Fig. 5.5. Kinematics of the system due to soil settlements.

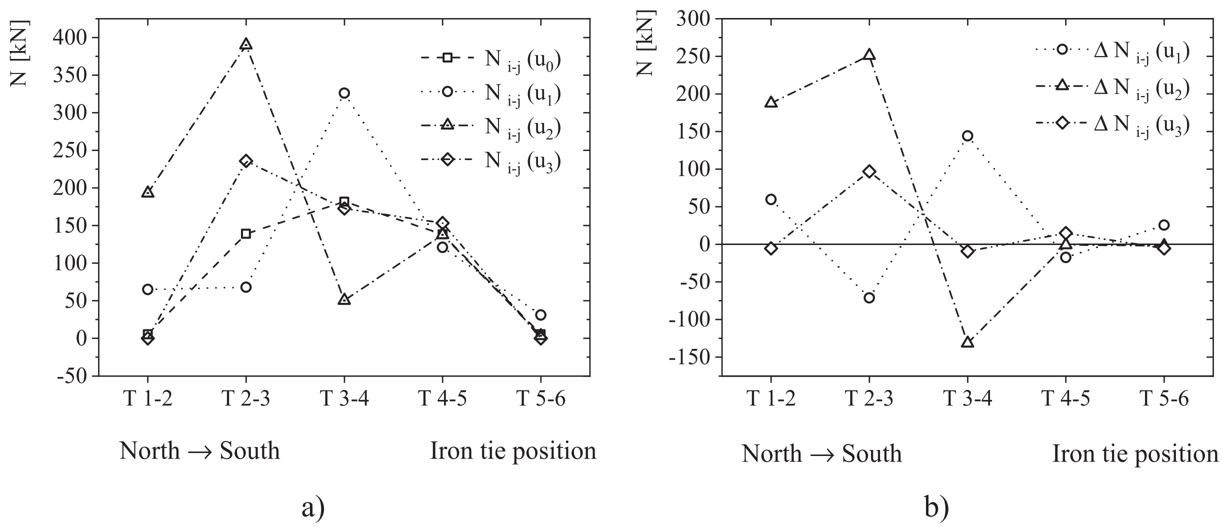

Fig. 5.6. Influence of support settlements acting on one side (e.g. northern part) on the axial force of the iron tie rods: (a) Axial force, $N_{i-j}(u_i)$, due to unitary settlements, (b) Axial force values increment $\Delta N_{i-j}(u_i)$ due to unitary settlements with respect to self-weight configuration.

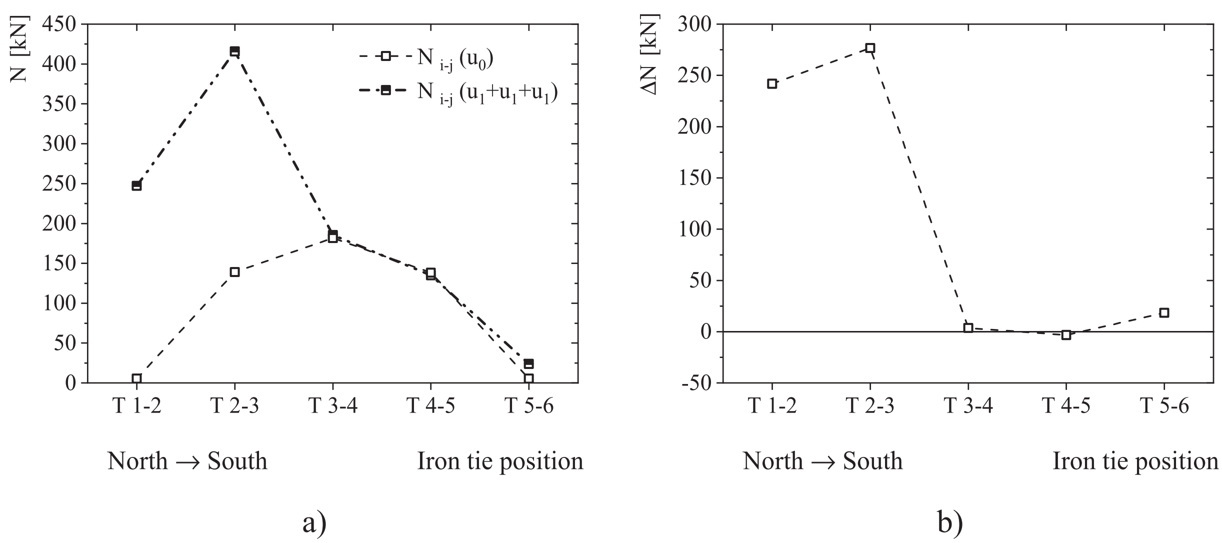

Fig. 5.7. The combination of the effects due to u_1, u_2 and u_3 compared to the self-weight (u_o) values: (a) Final value N_{i-j}, due to the combination, (b) Increments ΔN_{i-j}, with respect to self-weight configuration.

has a rather low effect in the iron ties axial force compared to the geometrical structural configuration of the cathedral or to differential soil settlements (as it will be explained in the following).

5.4. The effects of support settlements on the axial force in the iron tie rods

The effects of the supports are analysed by considering a unitary settlement of 1 cm, based on the soil settlements measured by Giussani and Roncoroni [37] over the last 50 years. Hence a vertical displacement is considered for each of the supports on the north side of the bay (P1, P2, P3). It is here noted that: u_i – are the values of the settlements in each pier, e.g. u_1, u_2 and u_3 are the settlement in the 1st, 2nd and 3rd pier respectively of the bay, object of study. While u_0 considers the case with no soil-settlements, $u_i = 0$.

Two aspects are analysed in the following:

(a) The kinematics produced in the system,
(b) The axial force development in iron ties.

(a) The considered vertical settlements u_i of each pier affects different portions of the structural system (see Fig. 5.5). Analysing the produced kinematics in the system it is possible to understand if the settlements will contribute to decreasing or increasing the axial force $N_{i-j}(u_i)$, in the iron ties. The simulations show that in general all the transversal section of the structure is affected by soil settlements, although the major displacements are typically observed only in the adjacent aisles to the applied settlement. Therefore, it is necessary to analyses the complete transversal section for realistic results.

(b) The new values of the tensile force in the iron ties due to each unitary settlement are plotted in Fig. 5.6a. The simulations show that each unitary settlement affects significantly the axial force in the iron ties, by increasing or decreasing the tensile force depending on the produced kinematics in the system (Fig. 5.6a). The computation of the difference between the settled state and the self-weigh configuration, $\Delta N_{i-j}(u_i)$, through Eq. (2) puts in evidence the contribution of each settlement (Fig. 5.6b).

$$\Delta N_{i-j}(u_i) = N_{i-j}(u_i) - N_{i-j}(u_0) \tag{2}$$

These results prove that soil settlements have an important contribution to the current measured values of the axial force. It is therefore carried forward in the following by further investigating the effect of soil settlements in the iron ties. It is shown in the following that a

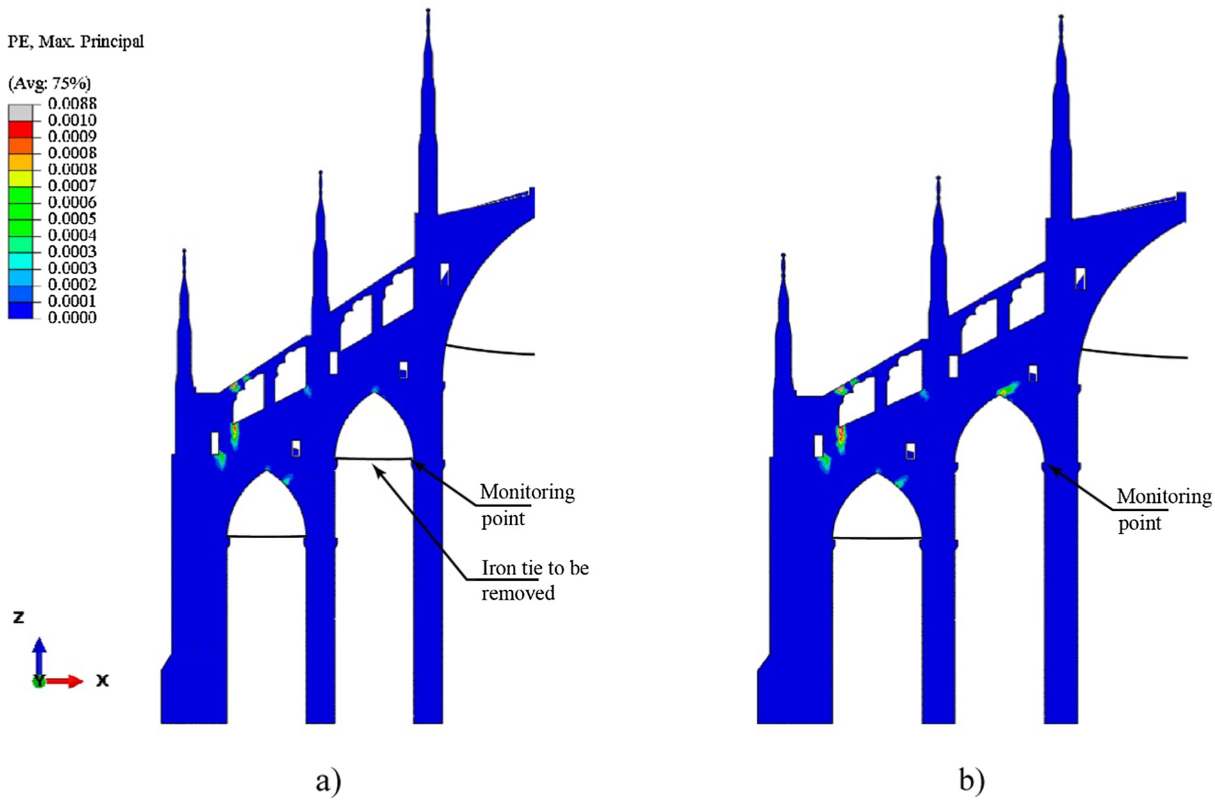

Fig. 5.8. Plot of plastic strains: (a) before and (b) after iron tie rod removal.

combination of the effects could arrive easily at failure point and therefore give us an insight on the observed tie breaks.

The measurements of soil settlement (see Section 3.2.4) show that the affected zone includes several piers. Hence, the experimentally measured tensile force in the iron ties is a result of the combination of single differential settlement developed in each pier. The settlements affect the self-weight state, $N_{i-j}(u_0)$, with the value, $\Delta N_{i-j}(u_i)$. As an approximation of the effects of the settlements, the following combination can be considered:

$$N_{i-j}(u) = N_{i-j}(u_0) + \alpha_1 \Delta N_{i-j}(u_1) + \alpha_2 \Delta N_{i-j}(u_2) + \alpha_3 \Delta N_{i-j}(u_3) \quad (3)$$

where: $i = 1, 2. ..n; j = i + 1.$ – integer number for supports between iron ties; $\alpha_1, \alpha_2, .., \cdots \alpha_i, .., \alpha_n$ – combination coefficients

The Eq. (3), is based on the combination of the axial force change $\Delta N_{i-j}(u_i)$ due to u_1, u_2 and u_3, with the self-weight axial force $N_{i-j}(u_0)$. Moreover, it is also necessary to understand the complex history of settlements up to the present stressed state of the iron ties. (Fig. 5.6, Fig. 5.7).

In particular, considering $\alpha_i = 1$ the following effects of the combinations are noted for each tie $T_{i\text{-}j}$ (Fig. 5.7):

(a) Side aisle tie ($T_{1\text{-}2}$ and $T_{5\text{-}6}$): The combination is a positive increasing function as all the settlements contribute by increasing the axial force in the iron ties located in the side aisle. Hence resulting in moderate values of axial force, up to 247 kN. The main contributor is u_2 with 188 kN per unitary settlement.
(b) Middle aisle tie ($T_{2\text{-}3}$ and $T_{4\text{-}5}$): The combination has mainly an increasing effect in function of the active settlement, with very high values around 416 kN. The main contributors are u_2 with 251 kN followed by u_3 with 97 kN per unitary displacement.
(c) Central nave tie ($T_{3\text{-}4}$): The settlement of the nave support (u_3) does not introduce any major change in the axial force, while settlements of the buttress (u_1) and pier (u_2) supports would cause a slight increase of only 4 kN in the axial force being of nearly the same order of magnitude. The computations show that the tie $T_{3\text{-}4}$ would have tension force resulting mainly as due to the contribution of the self-weight.

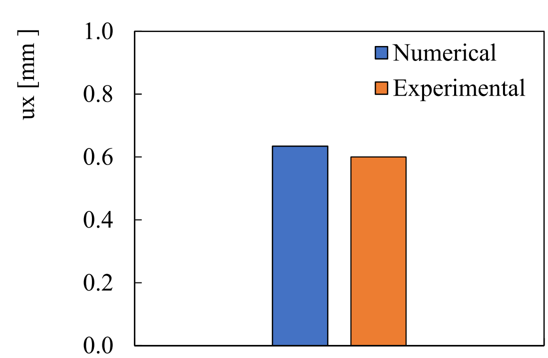

Fig. 5.9. Horizontal displacement of the pier top after tie rod removal.

The combination gives the highest effects in the 2nd bay, inducing an increase in the axial force $T_{2\text{-}3}$ from 182 kN up to 416 kN, equivalent to 230% of the initial value (Fig. 5.7).

As a general conclusion we expect elevated stresses in the side aisle iron ties ($T_{1\text{-}2}$ and $T_{5\text{-}6}$) and high probability of failure for the middle aisle ties ($T_{2\text{-}3}$ and $T_{4\text{-}5}$), while in the central nave we expect values close to the self-weight. As a matter of fact, the survey shows that most of the observed iron tie failures are located in the middle aisle ($T_{2\text{-}3}$ and $T_{4\text{-}5}$).

5.5. Maintenance operation: iron tie removal or failure

Another possible application of the developed modelling strategy are maintenance works, which in some cases include the replacement of damaged iron tie-rods. In the following it is considered a real replacement operation at Milan Cathedral, where the displacement of the pier during the replacement operation was experimentally measured [12,37].

The replacement of the tie rod is modelled numerically through the removal of the iron tie element from the global numerical model. The simulation shows that damage (plastic strain) due to the removal of one

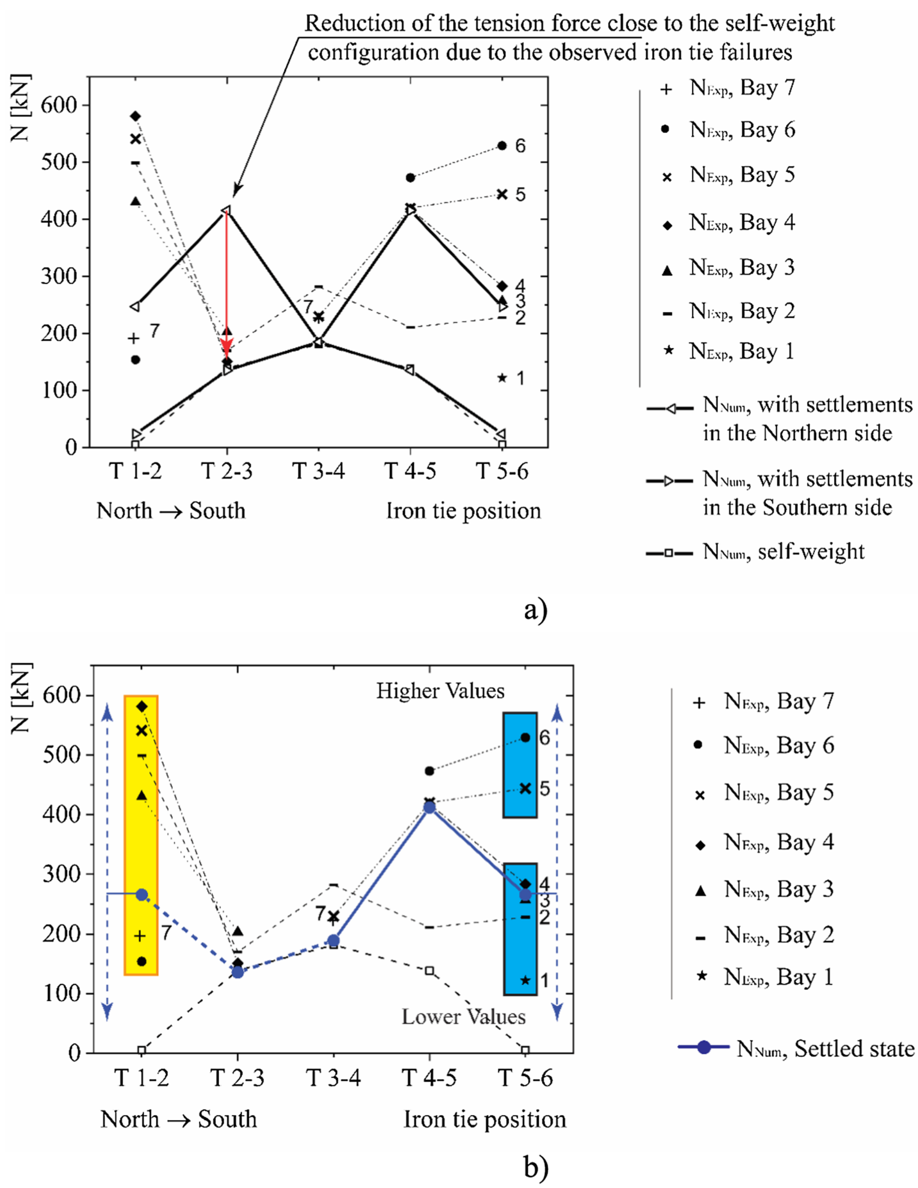

Fig. 6.1. Values of the axial force in the iron tie rods: (a) Initial symmetric prediction, without tension tie failure, (b) Final prediction with internal force redistribution due to the observed iron tie failure.

of the iron ties is rather limited (compare Fig. 5.8a and b), at least in short-term as no viscous effects are considered. However, these results match the limited damage experimentally observed in the cathedral. In the present research, very little or no-sign of particular damage is found in the locations where the tie-rod failure was documented.

The simulations predicted a 0.6 mm horizontal translation of pier top after the tie removal (Fig. 5.9), directed towards the nave (monitoring point in Fig. 5.8). The comparison of the simulation with the case of the removal of the tie rod $T_{2\text{-}3}$ (3rd bay) or the failure of the tie $T_{2\text{-}3}$ (6th bay) described by Giussani and Roncoroni [37], shows the same direction and displacement range (0.6–1.5 mm). The results confirm also the modelling accuracy of the numerical model, in terms of relative rigidity between structural members.

6. Discussion

In this section, a discussion is developed about the correlation between iron tie tension and soil settlements in the longitudinal direction of the naves. We recall that the experimentally measured non-symmetrical distribution of the forces in the iron ties (Fig. 5.1b) was previously related to soil settlements (see Section 3.2.4). Hence, we consider the hypothesis that the present state derives from a combination of soil settlements in each of the piers.

At an initial step, referring to a single bay, the distribution of tension forces in the ties is assumed as symmetrical between the northern and southern part. In each side, we can plot two analytical graphs considering the effects of differential soil settlements (Fig. 6.1a). Whereas the experimental values of the middle aisle tie $T_{2\text{-}3}$ and $T_{4\text{-}5}$ are not symmetrical (Fig. 6.1a). This is interpreted by a redistribution of forces in middle aisle tie $T_{2\text{-}3}$ caused by its break (see the case of bays 3-5-6), hence lowering the value of the tensile force close to the self-weight value (see red[1] arrow in Fig. 6.1a).

Evidence of the force redistribution can be found in the experimentally documented iron ties failures (3rd, 5th and 6th bay, in Fig. 3.7), which are located in the middle aisle ($T_{2\text{-}3}$). Hence a correction must be made in the numerical prediction by considering an

[1] For interpretation of color in Fig. 6.1, the reader is referred to the web version of this article.

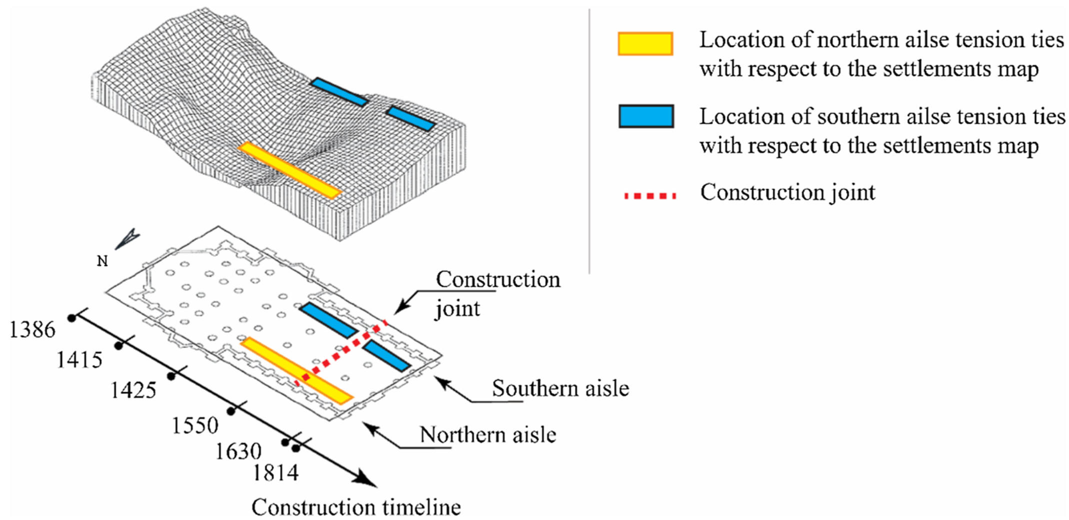

Fig. 6.2. Vertical displacements from the monitoring system for the period 1986–1998 according to Giussani and Roncoroni [37], correlated with the axial force prediction in the ties of the lateral aisles.

internal force redistribution, e.g. drop of the axial force increment due to settlements $\Delta N_{2-3}(u_i) = 277$ kN (Fig. 6.1a). Hence, the predicted numerical value is the same as in self-weight configuration, 139 kN. Therefore, this explains that the low scatter in the value of T_{2-3} (found in the range 151 kN–203 kN) is due to the failures that have taken place in these locations. After the replacement operation, experimentally measured tensions move close to the self-weight equilibrium values.

The final distribution of the tensile force in the iron ties considering the settlements is plotted in Fig. 6.1b. The numerical prediction shows a good correlation with the measured values in the two ties in the middle aisles, T_{2-3} and T_{4-5}, and the ties in the central nave, T_{3-4}. Regarding the two-remaining aisle ties, T_{1-2} (north aisle) and T_{5-6} (south aisle), from the numerical prediction in the northern and southern part, there is a variation moving from one bay to the other in the East-West directions; this occurs both on the South side and the North side (shown with dashed arrows in Fig. 6.1b). This is further supported by the higher settlements in the east side of the naves compared to the west side, which is relatively newer. The measured values of the aisle ties, T_{1-2} (north aisle) and T_{5-6} (south aisle) are analysed in the following:

In the longitudinal direction the data from the monitoring system highlight two areas with different range of settlements divided by sharp differential settlements in the proximity of the historic construction joint (see Fig. 6.2). In the southern aisle, where no iron tie failures are documented, it motivates a clear the division in two groups of the experimental values:

(a) lower values 122 kN–283 kN,
(b) higher values 444 kN–549 kN (see the two blue rectangles in Fig. 6.1b).

Older parts (in the east of the construction joint, Fig. 3.2), being subject to larger settlements have higher values of tension force in ties (Fig. 6.2). In contrary, newer parts (in the west side of the construction joint) are subject to lower settlements. Therefore, in the last case lower values of tensile forces are measured experimentally closer to the self-weight equilibrium state (Fig. 6.2). The situation in the southern part of the system is at an intermediate state with a linear distribution of experimental values of the tension force increasing from west to east, due to lower magnitude of differential settlements compared with the rest of the system and no observed tie failures (Fig. 6.2).

On the northern side, the tensile force values range is between 154 kN and 581 kN. Here, the division of the values in the proximity of the construction joint is not so clear in the present state due to the observed iron tie failures (see Fig. 3.7). The system here is in a rather more critical condition compared to the southern ties due to the already observed failure in the adjacent aisle, T_{2-3}.

To summarize, the final configuration would be a non-symmetric condition (graph in blue in Fig. 6.1b) with tie failure in the north middle aisle due to higher settlements and with elevated values of force in the tension ties in the side aisles (divided in two groups by the construction joint). On the south side of the cathedral nave are found lower values of tension forces due to the low magnitude of settlements which are not sufficient to cause the iron tie failure.

7. Conclusions

The aim of creating an efficient model for studying the response of complex historical buildings, to understand the causes of tie rod failures has been fulfilled. The process involves the use of experimental observations at several levels, in the setup of geometry, choice of material properties, definition of construction stages, measurement of tensile force of iron ties and definition of settlement scenarios imposed as actions on the structure. The present strategy to study the experimental tension forces of iron ties rods is illustrated in the case of Milan Cathedral. It clearly stands as a general procedure and therefore applicable to different historical buildings.

In the case of Milan Cathedral, the successful performance of the numerical model is shown by its correctly predicting and interpreting the experimental measurement of the axial force in function of the measured soil settlements. In particular the analysis concludes that after iron tie replacement, the experimentally measured tension forces tend to move to the self-weight equilibrium values, leading to lower scatter of data. On the other hand, large scatter of tension values infer that no recent iron tie failure has occurred. The present values results from a complex loading history which should be investigated considering different sources. The results show that the observed failures are due to a combination of effects, particularly the settlements which were observed in the 20th century. Taking advantage of the developed model, the effects of the soil settlements on the axial force were quantified. The analysis results show that the middle aisles are the most vulnerable locations where actually several failures were observed in the cathedral.

A sensitivity analysis was carried out to study the effects of the modelling choices (e.g. loading history and material properties) on the prediction of tension in the iron ties. The variation of material properties does not influence particularly the distribution of the tension forces. The consideration of the staged construction analysis was shown to give better results in terms of tension force prediction in the iron ties compared to the instantaneous application of the loads.

The utility of the research stands in the possibility to provide a mechanical interpretation of experimental measurements and predict the tie tension based on given settlements, which in return permits to provide insight in the safety of the structural system with iron tie rods. Moreover, the same numerical model can be used during maintenance and replacement of iron ties by precisely predicting the actual mechanical state in the tie and internal forces in the system. The current developed modelling strategy is here proposed as a basis for future maintenance, monitoring or interventions design in historical buildings.

Future research could focus on two directions: a) investigation of the long-term response or safety of the building related to the failure of one or more tie rods, not replaced when needed because of inadequate maintenance, and b) enriching the numerical model of the cathedral with the geotechnical part in order to investigate in detail the effects of the heterogeneous soil profile and water table movements on the measured settlements in each of the monitored piers.

Declaration of Competing Interest

The authors declared that there is no conflict of interest.

Acknowledgements

The authors would like to acknowledge the Veneranda Fabbrica del Duomo di Milano (VFD), in particular Ing. Francesco Canali for possibility to work in the Cathedral of Milan. We wish to thank Prof. Stefano Della Torre who supported the study of the Cathedral of Milan within the agreement between the Politecnico di Milano and the VFD.

References

[1] Heyman J. The stone skeleton. Int J Solids Struct 1966;2(2):249–79. https://doi.org/10.1016/0020-7683(66)90018-7.

[2] Viollet-le-Duc E-E. Dictionnaire raisonné de l'architecture française du XIe au XVIe siècle, vols. 10, Morel, Paris, p. 1854–68.

[3] Ungewitter GG, Mohrmann K. Lehrbuch der gotischen Konstruktionen. Weigel; 1892.

[4] Bork R, Montogmery S, De Vegvar CN, Shortell E, Walton SA. De re metallica: the uses of metal in the middle ages. Routledge; 2017. isbn:1351946153.

[5] Acland JH. Medieval structure: the gothic vault. University of Toronto Press; 1972. isbn:9780802018861.

[6] Carbonara G. Trattato di restauro architettonico. Utet; 1996. isbn:978-8802046693.

[7] Mora-Gómez J. Historical iron tie-rods in vaulted structures: parametrical study through a scaled model. WIT Trans Built Environ 2015;153:669–80https://www.witpress.com/Secure/elibrary/papers/STR15/STR15056FU1.pdf.

[8] Giuriani E. Consolidamento degli edifici storici: restauro e recupero. UTET scienze tecniche; 2012. isbn:8859807638.

[9] AlShawa O, Liberatore D, Sorrentino L. Dynamic one-sided out-of-plane behavior of unreinforced-masonry wall restrained by elasto-plastic tie-rods. Int J Arch Herit 2019;13(3):340–57. https://doi.org/10.1080/15583058.2018.1563226.

[10] Podestà S, Scandolo L. Earthquakes and tie-rods: assessment, design, and ductility issues. Int J Arch Herit 2019;13(3):329–39. https://doi.org/10.1080/15583058.2018.1563239.

[11] Ferrari da Passano C. Il Duomo rinato: Storia e tecnica del restauro statico dei piloni del tiburio del Duomo di Milano [in Italian]. Milan: Veneranda Fabbrica del Duomo (Diakronia); 1988.

[12] Vasic M. A multidisciplinary approach for the structural assessment of historical constructions with tie-rods; 2015. http://hdl.handle.net/10589/100384.

[13] Bellanova M. A multidisciplinary and multiscale strategy for the assessment of the structural safety of historical metallic tie-rods; 2017. http://hdl.handle.net/10589/132563.

[14] Angjeliu G. Integrated structural modelling and experimental observations in historic masonry constructions PhD Thesis Department of Civil and Environmental Engineering, Politecnico di Milano Milan (IT); 2018http://hdlhandle.net/10589/139005.

[15] Bati SB, Tonietti U. Experimental methods for estimating in situ tensile force in tie-rods. J Eng Mech-ASCE 2001;127(12):1275–83. https://doi.org/10.1061/(Asce)0733-9399(2001)127:12(1275).

[16] Lagomarsino S, Calderini C. The dynamical identification of the tensile force in ancient tie-rods. Eng Struct 2005;27(6):846–56. https://doi.org/10.1016/j.engstruct.2005.01.008.

[17] Collini L, Fagiani R, Garziera R, Riabova K, Vanali M. Load and effectiveness of the tie-rods of an ancient Dome: technical and historical aspects. J Cult Herit 2015;16(4):597–601. https://doi.org/10.1016/j.culher.2014.09.008.

[18] Coïsson E, Collini L, Ferrari L, Garziera R, Riabova K. Dynamical assessment of the work conditions of reinforcement tie-rods in historical masonry structures. Int J Arch Herit 2019;13(3):358–70. https://doi.org/10.1080/15583058.2018.1563231.

[19] Collini L, Garziera R, Riabova K. Vibration analysis for monitoring of ancient tie-rods. Shock Vib 2017;2017:1–11. https://doi.org/10.1155/2017/7591749.

[20] Cescatti E, Da Porto F, Modena C. Axial force estimation in historical metal tie-rods: methods, influencing parameters, and laboratory tests. Int J Arch Herit 2019;13(3):317–28. https://doi.org/10.1080/15583058.2018.1563234.

[21] Tullini N, Rebecchi G, Laudiero F. Reliability of the tensile force identification in ancient tie-rods using one flexural mode shape. Int J Arch Herit 2019;13(3):402–10. https://doi.org/10.1080/15583058.2018.1563227.

[22] Garziera R, Collini L. A non-destructive technique for the health monitoring of tie-rods in ancient buildings. Proc conference proceedings of the society for experimental mechanics. Jacksonville, Florida USA: Springer; 2011. p. 7–13.

[23] Garziera R, Amabili M, Collini L. A hybrid method for the nondestructive evaluation of the axial load in structural tie-rods. Nondestr Test Eval 2011;26(02):197–208. https://doi.org/10.1080/10589759.2011.556728.

[24] Amabili M, Carra S, Collini L, Garziera R, Panno A. Estimation of tensile force in tie-rods using a frequency-based identification method. J Sound Vib 2010;329(11):2057–67. https://doi.org/10.1016/j.jsv.2009.12.009.

[25] Gentile C, Poggi C, Ruccolo A, Vasic M. Vibration-based assessment of the tensile force in the tie-rods of the Milan Cathedral. Int J Arch Herit 2019;13(3):411–24.

[26] Angjeliu G, Coronelli D, Cardani G. Structural modelling of complex historic masonry buildings. Proc 10th international masonry conference, Milan, Italy. 2018. p. 229–44http://hdl.handle.net/11311/1079149.

[27] Cardani G, Coronelli D, Angjeliu G. Damage observation and settlement mechanisms in the naves of the Cathedral of Milan. Proc structural analysis of historical constructions (SAHC) Leuven, Belgium 2016. https://doi.org/10.1201/9781315616995-93.

[28] L'Heritier M. L'utilisation du fer dans l'architecture gothique: les cas de Troyes et de Rouen. Université Panthéon-Sorbonne-Paris I; 2007https://tel.archives-ouvertes.fr/tel-00295179.

[29] Bellanova M, Felicetti R. A multidisciplinary strategy for the inspection of historical metallic tie-rods: the Milan Cathedral case study. Int J Arch Herit 2019:1–19. https://doi.org/10.1080/15583058.2018.1563228.

[30] Ferrari da Passano C, Brivio E. Contributo allo studio del tiburio del Duomo di Milano: Alcune considerazioni maturate a seguito dei lavori di restauro. Arte lombarda 1967;12(1):3–36http://www.jstor.org/stable/43131702.

[31] Coronelli D, Caggioni B, Zanella F. The Cathedral of Milan: the structural history of the load-bearing system. Int J Arch Herit 2015. https://doi.org/10.1080/15583058.2013.821541.

[32] Angjeliu G, Coronelli D, Cardani G. Challenges in modelling complex geometry in historical buildings for numerical simulations. Cocchiarella L, editor. Proc the 18th international conference on geometry and graphics, vol. 809. Milan, Italy: Springer; 2019. p. 1218–30. https://doi.org/10.1007/978-3-319-95588-9_105.

[33] Angjeliu G, Cardani G, Coronelli D. A parametric model for ribbed masonry vaults. Autom Constr 2019;105:102785. https://doi.org/10.1016/j.autcon.2019.03.006.

[34] Angjeliu G, Cardani G, Coronelli D. Digital modelling and analysis of masonry vaults. ISPRS - Int Arch Photogramm Remote Sens Spat Inform Sci 2019;XLII-2/W11:83–9. https://doi.org/10.5194/isprs-archives-XLII-2-W11-83-2019.

[35] Coronelli D, di Prisco C, Pisanò F, Imposimato S, Ghezzi S, Pesconi M. The tiburio of the cathedral of Milan: Structural analysis of the construction & 20th century foundation settlements; 2014.

[36] Croce A. Antichi monumenti e città. Ricerca e conservazione. An overview. Geotechnical Engineering in Italy; 1985. p. 57–110.

[37] Giussani A, Roncoroni F. Relazione delle misure eseguite per il controllo delle deformazioni del Duomo di Milano nei anni 2009–2017 [Internal Report]. Italy: Laboratorio Gicarus, Polo Territoriale di Lecco, Politecnico di Milano; 2014.

[38] Niccolai C. Il sottosuolo del territorio di Milano. Rivista Italiana di Geotecnica 1967;1:7–33http://www.associazionegeotecnica.it/rig/1967/1/il-sottosuolo-del-territorio-di-milano.

[39] Ferrari da Passano C. Interventi di consolidamento delle strutture del duomo di milano a seguito di fenomeni di subsidenza. Atti del xiv convegno nazionale di geotecnica, firenze, 28–31 ottobre 1980. Associazione geotecnica italiana; 1980. p. 177–86.

[40] Hibbitt, Karlsson, Sorensen. ABAQUS manual. Dassault Systèmes; 2016.

[41] Zienkiewicz OC, Taylor RL, Zienkiewicz OC, Taylor RL. The finite element method. London: McGraw-hill; 1977. isbn:ISBN- 13: 978-0470395066.

[42] Lubliner J, Oliver J, Oller S, Onate E. A plastic-damage model for concrete. Int J Solids Struct 1989;25(3):299–326. https://doi.org/10.1016/0020-7683(89)90050-4.

[43] Lee JH, Fenves GL. Plastic-damage model for cyclic loading of concrete structures. J Eng Mech-ASCE 1998;124(8):892–900. https://doi.org/10.1061/(Asce)0733-9399(1998)124:8(892).

[44] Abdelmoneim Elamin Mohamad A-B, Chen Z. Experimental and numerical analysis of the compressive and shear behavior for a new type of self-insulating concrete masonry system. Appl Sci 2016;6(9):245.

[45] Agnihotri P, Singhal V, Rai DC. Effect of in-plane damage on out-of-plane strength of unreinforced masonry walls. Eng Struct 2013;57:1–11. https://doi.org/10.1016/j.engstruct.2013.09.004.

[46] Aref AJ, Dolatshahi KM. A three-dimensional cyclic meso-scale numerical procedure for simulation of unreinforced masonry structures. Comput Struct 2013;120:9–23. https://doi.org/10.1016/j.compstruc.2013.01.012.

[47] Borri A, De Maria A. Linee guida per la compilazione della scheda di valutazione dell'IQM. Rete dei Laboratori Universitari di Ingegneria Sismica (RELUIS); 2005. Progetto esecutivo 2008.

[48] Roca P, Cervera M, Pelà L, Clemente R, Chiumenti M. Continuum FE models for the analysis of Mallorca Cathedral. Eng Struct 2013;46:653–70. https://doi.org/10.1016/j.engstruct.2012.08.005.

[49] Vannucci P, Masi F, Stefanou I. A nonlinear approach to the wind strength of Gothic Cathedrals: the case of Notre Dame of Paris. Eng Struct 2019;183:860–73. https://doi.org/10.1016/j.engstruct.2019.01.030.

[50] Van der Pluijm R, Rutten H, Ceelen M. Shear behaviour of bed joints. Proceedings of the twelfth international brick/block masonry conference, Madrid, Spain, vol. 3. 2000. p. 1849–62.

[51] Lourenco PB. Computational strategies for masonry structures. TU Delft, Delft University of Technology; 1996. isbn:9040712212.

[52] Page A. An experimental investigation of the biaxial strength of brick masonry. Proceedings of the sixth international brick masonry conference, Rome. 1982. p. 3–15.

[53] Dhanasekar M, Kleeman PW, Page AW. Biaxial stress-strain relations for brick masonry. J Struct Eng-ASCE 1985;111(5):1085–100. https://doi.org/10.1061/(Asce)0733-9445(1985)111:5(1085).

[54] Naraine K, Sinha S. Stress-strain curves for brick masonry in biaxial compression. J Struct Eng 1992;118(6):1451–61. https://doi.org/10.1061/(asce)0733-9445(1992)118:6(1451).

[55] Pelà L, Bourgeois J, Roca P, Cervera M, Chiumenti M. Analysis of the effect of provisional ties on the construction and current deformation of Mallorca Cathedral. Int J Arch Herit 2014;10(4):418–37. https://doi.org/10.1080/15583058.2014.996920.

[56] Augenti N, Parisi F. Experimental data analysis on mechanical parameters of tuff masonry. Proc second workshop on design for rehabilitation of masonry structures, Polistampa, Ischia, Italy. 2009. isbn:978-8859611417.

[57] Saloustros S, Pelà L, Contrafatto FR, Roca P, Petromichelakis I. Vulnerability assessment of monumental masonry structures including uncertainty, vol. 18; 2019, p. 1219–28. https://doi.org/10.1007/978-3-319-99441-3_131.

[58] Calderini C, Piccardo P, Vecchiattini R. Experimental characterization of ancient metal tie-rods in historic Masonry Buildings. Int J Arch Herit 2019;13(3):425–37. https://doi.org/10.1080/15583058.2018.1563230.